

A new method for automatic border detection in IVUS images and 3D visualization of segmented frames

Z.Najafi¹, A.Taki^{1,2}, K.Setarehdan¹, R.Zoroofi¹, A. Konig³ and N.Navab²

1 Faculty of Electrical and Computer Engineering, University of Tehran, Iran

2 Computer Aided Medical Procedures (CAMP) - TU Munich, Germany

3 Medizinische Poliklinik Innenstadt Klinikum der Universitat Mnchen, Germany

Keywords: Deformable model, IVUS, Border detection, Visualization.

Abstract—In this paper, we present a method for the automated detection of lumen and media–adventitia border in intravascular ultrasound (IVUS) images. The method is based on non-parametric deformable models for accurate IVUS image segmentation. The proposed method is evaluated using 50 IVUS frames from 10 patients. The obtained results demonstrate that our method is statistically accurate and capable to identify boundaries automatically. In IVUS images Calcified deposits appear as bright echoes between two detected borders and obstruct the penetration of ultrasound, a phenomenon known as “acoustic shadowing.” We visualized the segmented frames and highlighted the calcified regions in the 3D representation of IVUS images.

1 Introduction

Intravascular Ultrasound (IVUS) is a catheter-based medical imaging technique. Using a specially designed ultrasound catheter it provides real-time tomographic images of the arterial wall that shows the morphology and histological properties of a cross-section of the vessel. IVUS not only provides a quantitative assessment of the vessels' wall but also introduces information about the nature of atherosclerotic lesions as well as the plaque shape and size [1], [2]. The first step for plaque characterization is segmentation and processing of IVUS images and with a better segmentation we will have a better classification. Nevertheless, it is a difficult, subjective and time-consuming procedure to perform the analysis of segmentation manually. Therefore, there is an increasing interest in developing automatic tissue segmentation algorithms for IVUS images [3]. Several algorithms for lumen and media-Adventitia contours detection have been reported in the last decade. Various edge detection and contour identification techniques together with different border optimization algorithms such as dynamic programming, graph searching, simulated annealing, solution of partial differential equations, and genetic algorithms have been applied to the IVUS images in these articles [4], [5].

Recent approaches are mostly based on the active contours together with minimizing an energy or cost function which guides a snake towards the vessel borders.

The active contours used in the previous approaches are mostly based on a kind of parametric deformable model. However, parametric deformable models have two main limitations. First, in situations where the initial model and desired object boundary differ greatly in size and shape, the model must be re-parameterized dynamically to faithfully recover the object boundary. The second limitation is that it has difficulty dealing with topological adaptation such as splitting or merging model parts, a useful property for recovering either multiple objects or objects with unknown topology [6].

In this work, we focus on the development and validation of an automated method based on non-parametric deformable models for accurate IVUS image segmentation.

While IVUS images are noisy and the actual boundaries of regions of interest are difficult to be identified in many cases, it is essential to perform a denoising method before any edge detection algorithm. Many methods are known to be useful in smoothing noisy images. In this research anisotropic diffusion is used to preserve and to enhance edges in IVUS images.

The non-parametric models (also referred to as geometric deformable models) are used for boundary detection. These models are based on the curve evolution theory and the level set method. It provides an elegant solution to address the above mentioned primary limitation of the parametric deformable models. Other advantages of the geometric deformable models compared to parametric formulation include: (1) no parameterization of the contour, (2) topological flexibility, (3) good numerical stability, and (4) straightforward extension of the 2D formulation to n-D. The results of the application of the proposed algorithm to real IVUS images of different patients are presented and compared with snake methods.

Fibrous or calcified tissues are relatively echogenic. Calcium obstructs ultrasound penetration, obscuring the underlying vessel wall (acoustic shadowing; Figure 1). After identifying the plaque region that is between the detected borders,

visualized the segmented frames in 3D form and highlight the calcified regions.

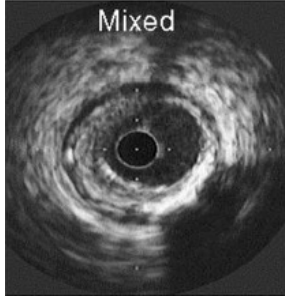


Fig.1.Mixed Fibrous and Calcified (shadowing)

2 Method

2.1 Pre Processing

In medical ultrasonic images like IVUS, edges and local details are the most interesting part for cardiologists. Therefore, to preserve and to enhance edges and local details on denoising are very important.

A feature preserving ultrasonic image denoising is put forth, which includes the anisotropic diffusion, which is controlled by the optimum smoothing time. The anisotropic diffusion is governed by the local coordinate transformation and the first and the second order normal derivatives of the image [7].

The operators of this class are capable of smoothing images without blurring the boundaries between their homogeneous regions. One choice is to use the following affine invariant anisotropic smoothing filter:

$$\frac{\partial I(x,y,t)}{\partial t} = \left[\left(\frac{\partial I}{\partial y} \right)^2 \frac{\partial^2 I}{\partial x^2} - 2 \frac{\partial I}{\partial x} \frac{\partial I}{\partial y} \frac{\partial^2 I}{\partial x \partial y} + \left(\frac{\partial I}{\partial x} \right)^2 \frac{\partial^2 I}{\partial y^2} \right]^{1/3} \quad (1)$$

Here $I(x, y, t)$ represents the image to be filtered, which is now considered to be a function of two spatial coordinates x and y , as well as of time t . It can be shown, that the above equation involving only the first and second order spatial derivatives of the image I defines the affine geometric heat flow, under which the level sets of I undergo affine curve shortening. Moreover, such a diffusion process has the desirable characteristics of preserving edges while exhibiting numerical stability and straightforward computation [8].

2.2 Borders Detection

Manual processing of IVUS images is a tedious and time consuming procedure. A lot of effort has been made in order to develop an accurate automated method for the detection of the regions of interest in IVUS images.

Many restrictions in automated segmentation of IVUS images derive from the quality of the image, such as the lack

of homogeneity of regions of interest and shadowed regions, which are produced by the presence of calcium.

In this work, we focus on the development and validation of automated methods based on deformable models for accurate IVUS image segmentation[8], [9].

2.2.1 Geometric Deformable Models

In the second stage of the proposed algorithm, the Geometric deformable model scheme is used for vessel boundary detection [10], [11].

Let us consider a dynamic curve as $X(s,t)=[X(s,t),Y(s,t)]$ where t is the time and s is the curve parameter. Let us also to denote the curve's inward unit normal as N and its curvature as κ . The evolution of the curve along its normal direction can be characterized by the following partial differential equation:

$$\frac{\partial X}{\partial t} = V(\kappa)N \quad (2)$$

$V(\kappa)$ is speed function since it determines the speed of the curve evolution. In the level set method, the curve is represented implicitly as a level set of a 2D scalar function which is usually defined on the same domain as the image itself. The level set is defined as the set of points that have the same function value.

We now derive the level set embedding of the curve evolution equation (1). Given a level set function $\phi(x,y,t)$ with the contour $X(s,t)$ as its zero level set we have:

$$\phi[X(s,t),t] = 0 \quad (3)$$

Differentiating the above equation with respect to t and using the chain rule, we obtain:

$$\frac{\partial \phi}{\partial t} + \nabla \phi \frac{\partial X}{\partial t} = 0 \quad (4)$$

Where $\nabla \phi$ denotes the gradient of ϕ , assuming that ϕ is negative inside the zero level set and positive outside it. Accordingly, the inward unit normal to the level set curve is given by

$$N = -\frac{\nabla \phi}{|\nabla \phi|} \quad (5)$$

Using Eqs. (1) and (4), the Eq. (3) can be rewritten as:

$$\frac{\partial \phi}{\partial t} = V(\kappa)|\nabla \phi| \quad (6)$$

Where κ the curvature at the zero level set is given by:

$$\kappa = \nabla \cdot \frac{\nabla \phi}{|\nabla \phi|} = \frac{\phi_{xx}\phi_y^2 - 2\phi_x\phi_{xy} + \phi_{yy}\phi_x^2}{(\phi_x^2 + \phi_y^2)^{3/2}} \quad (7)$$

The relationship between Eq. (2) and Eq. (6) provides the basis for performing curve evolution using the level set method. Since the evolution equation (6) is derived for the zero level set only, the speed function $V(\kappa)$, in general, is not defined on other level sets. Hence, we need a method to extend the speed function $V(\kappa)$ to all of the level sets. A speed function that is used by geometric deformable contours, takes the following form:

$$\frac{\partial \phi}{\partial t} = c(\kappa + V_0)|\nabla \phi| \quad (8)$$

Where

$$c = \frac{1}{1 + |\nabla(G_\sigma * I)|} \quad (9)$$

A positive value of V_0 shrinks the curve while a negative V_0 expands it. The curve evolution is coupled with the image data through a multiplicative stopping term. This scheme can work well for objects that have good contrast. However, when the object boundary is indistinct or has gaps like the IVUS image in our case, the geometric deformable contour may leak out because the multiplicative term only slows down the curve near the boundary rather than completely stopping the curve. Once the curve passes the boundary, it will not be pulled back to recover the correct boundary.

To overcome this deficiency a new term is added to Eq.(9) as shown in Eq.(10).

$$\frac{\partial \phi}{\partial t} = c(\kappa + V_0)|\nabla \phi| + \nabla c \nabla \phi \quad (10)$$

The resulting speed function has an extra stopping term $\nabla c \nabla \phi$ that can pull back the contour if it passes the boundary.

3 Results

In this work, we used a data set provided by a local hospital that includes 50 IVUS frames obtained from 10 different patients.

The level set based method was applied to each frame to detect intima layer by defining a circle of radius 1.5 times larger than radius of the catheter located at the centre of the image and can be located easily due to its clearly different contrast with the surrounding region.

A negative value is assigned for V_0 in equation (9) in order to expand the curve after some iteration to locate the Intimia boundary. Figure 2 shows an example outcome of the method. At the next step, considering a large circle whose diameter is as large as the diameter of the IVUS image itself and with a positive value for V_0 the curve shrinks to the Media- Adventitia layer after some iteration as shown in Figure 3.

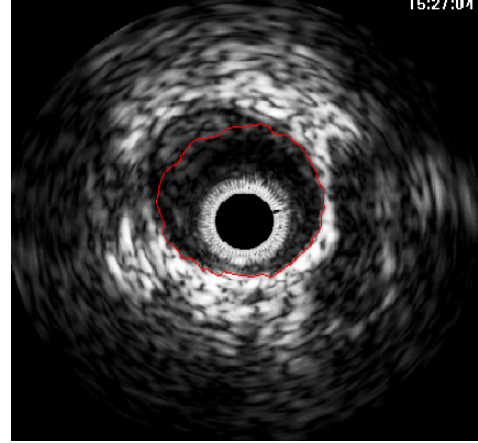


Fig. 2. Intimia border Detection

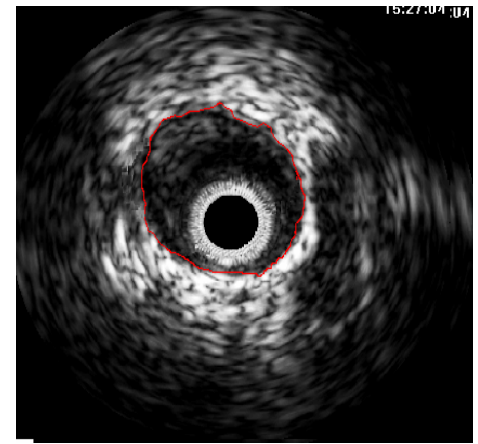


Fig. 3. Media-Adventitia border Detection

These results were compared to the boundaries manually identified by an expert cardiologist. The sensitivity and specificity of the proposed method were measured based on the occurrence of true positive and false positive (TP and FP, respectively), and true negative and false negative (TN and FN) results as follows:

$$\text{Sensitivity} = \text{TP} / (\text{TP} + \text{FN})$$

$$\text{Specificity} = \text{TN} / (\text{TN} + \text{FP})$$

The sensitivity for a class is the percentage of members of that class that are correctly defined by the test while the specificity for a class is the percentage of members of the other classes that are correctly classified by the test.

The resulting sensitivity and specificity of the proposed algorithm are 72% and 78% respectively.

After detecting these two borders we identify the calcified regions. The regions in frames which have shadow behind a white area, is the place that calcium or hard plaque is accumulated [12]. By finding these regions in a sequence of IVUS segmented images we can visualize them with VTK (Visualization Toolkit) software. Accumulated plaques between the two detected borders can be seen In Figure 4.

Figure 5 is the illustration of calcified regions in our visualization step.

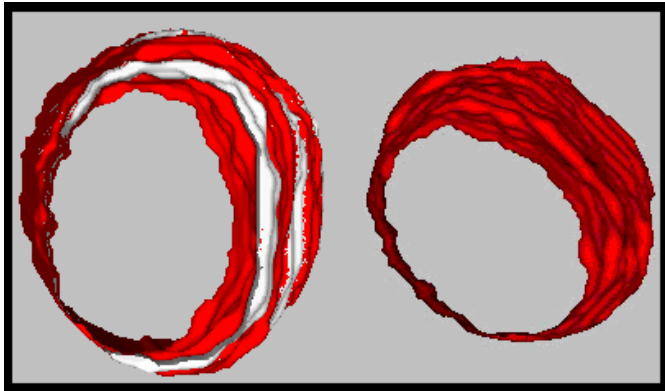


Fig. 4. Top view of 3D representation of detected borders and the plaques between these layers.

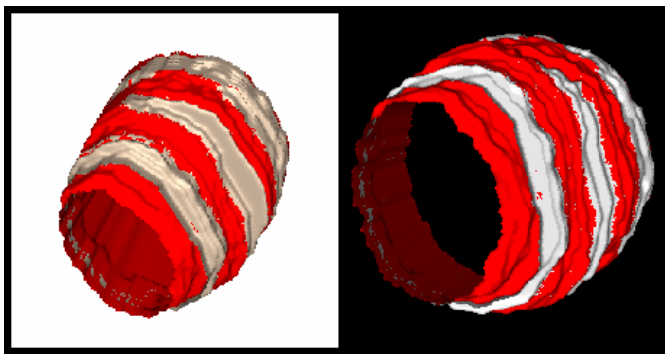


Fig. 5. Calcified regions in 3D visualized form in a part of vessel wall

4 Conclusion

Vessel border detection is of special interest for plaque assessment and quantification of lumen narrowing in IVUS images. In this paper, we propose a new automatic algorithm for vessel border detection in IVUS images based on the geometric deformable models to detect Intimial and Medial-adventitial borders. The inner and outer arterial wall boundaries generated by our segmentation algorithm are close to those manually identified by an IVUS expert.

References

- [1] D. Gil , A. Hernández, O. Rodriguez, J. Mauri, and P. Radeva, "Statistical Strategy for Anisotropic Adventitia Modelling in IVUS, "IEEE transaction on medical imaging, vol. 25, no. 6, June 2006.
- [2] E. dos filho , M. Yoshizawa, "A Study on Intravascular Ultrasound Image Processing, "Journal of Mathematical Imaging and Vision 21: 205–223, 2004.
- [3] D. Gil , A. Hernández, O. Rodriguez, J. Mauri, and P. Radeva, "Statistical Strategy for Anisotropic Adventitia

Modelling in IVUS, "IEEE TRANSACTIONS ON MEDICAL IMAGING, VOL. 25, NO. 6, JUNE 2006

- [4] M. Vavuranakis, C. Stefanidis, "Advanced in the detection of the vulnerable Coronary Atherosclerotic plaque, "Hellenic Journal cardiology, vol. 44, pp. 1-8, March 2003.
- [5] Z. Luo, Y. Wang, W. Wang, "Estimating Coronary Artery Lumen Area With Optimization-Based Contour Detection, "IEEE transaction on medical imaging, vol. 22, no. 4, pp 48-56. April 2003.
- [6] T. McInerney, and D. Terzopoulos, "Deformable models in medical image analysis: a survey, " Medical Image Analysis, 1, pp. 91-108, 1996.
- [7] J. Weickert, B. Romery, and M. Viergever, "Efficient and reliable schemes for nonlinear diffusion filtering," IEEE Trans. Image Processing, vol. 7, pp. 398–410, 1998.
- [8] S. Osher and J. A. Sethian, "Fronts propagating with curvature-dependent speed: algorithms based on Hamilton-Jacobi formulations," J. Computational Physics, vol. 79, pp. 12–49, 1988.
- [9] J. A. Sethian, "Curvature and evolution of fronts, "Commun. Math. Phys., vol. 101, pp. 487–499, 1985.
- [10] Xiao Han, Chenyang Xu, Jerry L. Prince, "A Topology Preserving Level Set Method for Geometric Deformable Models, "IEEE TRANSACTIONS ON PATTERN ANALYSIS AND MACHINE INTELLIGENCE, VOL. 25, NO. 6, JUNE 2003.
- [11] Jasjit S. Suri, Kecheng Liu, Sameer Singh, Swamy N. Laxminarayan, Xiaolan Zeng, and Laura Reden , "Shape Recovery Algorithms Using Level Sets in 2-D/3-D Medical Imagery: A State-of-the-Art Review, "IEEE TRANSACTIONS ON INFORMATION TECHNOLOGY IN BIOMEDICINE, VOL. 6, NO. 1, MARCH 2002.
- [12] G. S. MINTZ, S.E. NISSEN, "American College of Cardiology Clinical Expert Consensus Document on Standards for Acquisition, Measurement and Reporting of Intravascular Ultrasound Studies (IVUS), "Journal of the American College of Cardiology Vol. 37, No. 5.